



## **Supplementary Information for**

### **SNARE Machinery Is Optimized For Ultra-fast Fusion**

**Fabio Manca, Frederic Pincet, Lev Truskinovsky, James E. Rothman, Lionel Foret and Matthieu Caruel**

**Matthieu Caruel.**

**E-mail: [matthieu.caruel@u-pec.fr](mailto:matthieu.caruel@u-pec.fr)**

#### **This PDF file includes:**

Supplementary text

Figs. S1 to S2

References for SI reference citations

## Supporting Information Text

**A. Calibration of the SNAREpin model.** To calibrate and validate the model of a single SNAREpin, we use available experimental data on single molecule unfolding, see Refs. (1),(2). In this type of experiments, a single SNARE complex is attached to one bead and linked to another bead by a DNA handle. Both beads are trapped by optical tweezers. Increasing the distance between the two laser beams while recording the distance between the beads allows to measure the statistics of the fluctuations associated with unfolding events. Each event is characterized by finite size back and forth jumps of the bead's position, see Fig. S1 (blue trace).

A mechanical model of this experiment is shown in Fig. S2 (A). We take as a reference the position of the left bead to which the SNARE complex is directly attached (not drawn). The other end of the SNAREpin—whose position is denoted by  $y$ —is attached to the other bead via a DNA handle. This second bead, whose recorded position is denoted by  $y_B$  is trapped by a laser beam located at a controlled distance  $y_T$  from the reference.

The total energy of the system is given by

$$e(y, y_B; y_T) = e_{n,c}(y) + e_{\text{DNA}}(y, y_B) + e_T(y_B; y_T), \quad [1]$$

where,  $e_{n,c}(y)$  is the energy of the SNAREpin defined by Eq. (7) in Materials and Methods,  $e_{\text{DNA}}(y, y_B)$  is the energy of the DNA handle and  $e_T(y_B)$  is the energy associated with a displacement of the bead from the center of the optical trap. At the elongation where the  $n \leftrightarrow c$  transitions are observed, we can assume that the energies of both the DNA handle and the optical are quadratic. Denoting by  $\kappa_{\text{DNA}}$  and  $\kappa_T$  the stiffnesses of the DNA the optical trap, respectively, we have  $e_{\text{DNA}} = \frac{\kappa_{\text{DNA}}}{2}(y_B - y)^2$  and  $e_T = \frac{\kappa_T}{2}(y_T - y_B)^2$ .

**A.1. Estimation of the parameters  $a$  and  $e_0$ .** The total elongation  $y_T$  being fixed, the equilibrium distribution of the variable  $y_B$  takes the form

$$\rho(y_B) = \frac{1}{Z} \left\{ e^{-\frac{\tilde{e}_c(y_B)}{k_B T}} + e^{-\frac{\tilde{e}_n(y_B)}{k_B T}} \right\} e^{-\frac{e_T(y_B)}{k_B T}}, \quad [2]$$

where  $Z$  is the partition function,  $\tilde{v}_c(y_B) = \frac{1}{2}\tilde{\kappa}_c y_B^2$  and  $\tilde{v}_n(y_B) = e_0 + \frac{1}{2}\tilde{\kappa}_n(y_B - a)^2$ . The parameters

$$\tilde{\kappa}_{n,c} = \frac{\kappa_{n,c}\kappa_{\text{DNA}}}{\kappa_{\text{DNA}} + \kappa_{n,c}} \quad [3]$$

represent the equivalent stiffnesses of the SNARE and the DNA handles connected in series.

The fit of Eq. 2 to the experimental distribution of Ref. (1) [see Fig. S2(B)] is obtained with the following parameters:  $y_T = 992$  nm,  $a \sim 6.9$  nm,  $e_0 = 30.7$  k<sub>B</sub>T,  $\tilde{\kappa}_c \simeq 0.795$  pN nm<sup>-1</sup>, and  $\tilde{\kappa}_n \simeq 0.761$  pN/nm. The good agreement between the model and the data seems to validate our model, however, only indirect estimates of the stiffnesses of the stiffnesses  $\kappa_n$  and  $\kappa_c$  can be obtained at this stage because the distribution Eq. Eq. (2) only depends on the effective stiffnesses  $\tilde{\kappa}_{n,c}$ . This point is discussed in more details in the next section.

**A.2. Stiffness of the  $V_c$  domain,  $\kappa_c$ .** To identify the contribution of the SNAREpin stiffness to the parameters  $\tilde{\kappa}_{n,c}$ , we used the force *vs* extension response recorded with the DNA handle alone with the same setup. The force-extension curves obtained for DNA alone and for the SNAREpin + DNA system are superimposed in Fig. S1.

In the enthalpic regime, the DNA force-extension relation  $f(y_B)$  can be modeled as an extended worm-like chain (EWLC) (3, 4)

$$y_B = \ell_c \left[ 1 - \frac{1}{2} \left( \frac{\ell_p f(y_B)}{k_B T} - \frac{1}{32} \right)^{-\frac{1}{2}} + \frac{f(y_B)}{f_0} \right], \quad [4]$$

where the contour length of the DNA handle is  $\ell_c = 768$  nm (1), the persistent length  $\ell_p = 45$  nm (1), and  $f_0 = 560$  pN is a fitting parameter, chosen in agreement with the typical range of value adopted in literature (4). The force-extension curve obtained with this model is shown with the pink dashed line in Fig. S1. With these parameters, we estimate the DNA stiffness at the force  $f_* = 17$  pN—where the  $n \leftrightarrow c$  transition is observed—to be  $\kappa_{\text{DNA}} \simeq 0.4555$  pN nm<sup>-1</sup>.

We can now estimate the value of  $\tilde{\kappa}_c$  by using Eq. (4) with the SNARE+DNA system. In this case, the parameters are  $\ell_c = 768 + 2 = 770$  nm,  $\ell_p = 45$  nm and  $f_0 = 530$  pN. We obtain  $\tilde{\kappa}_c \simeq 0.4388$  pN nm<sup>-1</sup> (at  $f_* = 17$  pN). Notice that, the contour length has been increased by 2 nm to take into account the linker domain [see Ref. (1) for the details]. Finally, using Eq. 3, we obtain the following estimate for the stiffness of  $V_c$  domain (at the transition force):  $\kappa_c \simeq 12$  pN nm<sup>-1</sup>.

**A.3. Stiffness of the  $V_n$  domain,  $\kappa_n$ .** The same procedure cannot be used to estimate the value of  $\kappa_n$  because the  $n \leftrightarrow c$  transition is almost immediately followed by a large debonding which leaves a too short (about  $\sim 7$  nm) interval for identifying elastic properties, see Fig. S1. However, once the values of  $\kappa_c$  and  $e_0$  are fixed, the value  $\kappa_n$  directly controls the value of the intrinsic energy barrier  $\Delta e$  and therefore the value of  $\Delta\Phi_1$  ( $N = 1$ ), see the paragraph preceding Eq. (6) in the main text. The estimate  $\Delta\Phi_1 \sim 0$  k<sub>B</sub>T to 4.7 k<sub>B</sub>T was obtained in Refs. (1, 5) from the analysis of the of the  $n \leftrightarrow c$  transition kinetics. We chose the intermediate value of  $\Delta v = 2$  k<sub>B</sub>T, corresponding to  $\kappa_n \simeq 2.5$  pN nm<sup>-1</sup>, and we performed a complementary parametric study for different values of  $\Delta v$  in the broad range of 0 – 11 k<sub>B</sub>T (see Fig 3 of the main text).

**B. Parameters of the Fusion Energy Barrier.** We interpret the reference  $y = 0$  as a state where the two fully dehydrated membranes would be in contact, with the SNAREs being fully zippered. The two membranes remain stable as long their distance is above  $\sim 2$  nm, see (6, 7). Therefore we fix the position of the fusion point at  $y_f = 2$  nm. The typical range of the repulsive forces is  $\sigma_f \simeq 0.3$  nm, in accordance with Refs. (8, 9).

For the height of the fusion barrier  $e_f$ , a broad range of value, from  $20 k_B T$  to  $35 k_B T$ , can be found in the literature, see (10–21). This number depends on the type of lipid, and on the curvature and tension of the membranes (16–20). Recent experiments measuring the spontaneous fusion rate of lipid vesicles *in vitro* lead to the estimate  $e_f = 26\text{--}34 k_B T$  depending on the lipid type (15). In our simulations (see Fig. 2 in the main text), we set  $e_f = 26 k_B T$ , which corresponds to the value reported for POPC (1-palmitoyl-2-oleoyl-sn-glycero-3-phosphocholine) membranes. With this value, the average fusion time is 1 s for  $N = 1$  as measured in Ref. (21, 22). A parametric study of the influence of the value of  $e_f$  is discussed in the main text.

**C. Numerical implementation of the model.** The overdamped Langevin dynamics of the vesicle (see Eq. (1) of the main text) is simulated using a first-order integrator of the overdamped Langevin equation (23). At each time step  $i$ , the new position of the vesicle membrane  $y^{i+1}$  is computed as follows

$$y^{i+1} = y^i - \frac{\Delta t}{\eta} \frac{\partial}{\partial y} [E_{\text{snare}}(y, N_c) + E_{\text{fusion}}(y)] \Big|_{y^i, N_c^i} \sqrt{\frac{2k_B T}{\eta} \Delta t} \xi^i, \quad [5]$$

where  $\xi^i$  is a random number drawn from the standard normal distribution. We consider  $k^{-1}$  as the time scale of the system, and fixed  $\Delta t = 4.5 \times 10^{-3} k^{-1}$ .

The value  $N_c^{i+1}$  is obtained by writing  $N_c^{i+1} = N_c^i + \Delta N_c^i$ , with the increment  $\Delta N_c^i$  given by

$$\Delta N_c^i = \begin{cases} +1 & \text{if } r^i < W_+^i \Delta t, \\ -1 & \text{if } W_+^i \Delta t \leq r^i < (W_+^i + W_-^i) \Delta t, \\ 0 & \text{otherwise,} \end{cases}$$

where  $r^i$  is a random number uniformly distributed in the interval  $[0, 1]$ . The transition rates  $W_{\pm}^i$  are defined by  $W_+^i = (N - N_c^i) k_+(N_c^i, y^{i+1})$  and  $W_-^i = N_c^i k_-(N_c^i, y^{i+1})$ . To obtain the statistics presented in the main text,  $10^3$  realizations of this process have been generated with the same initial condition.

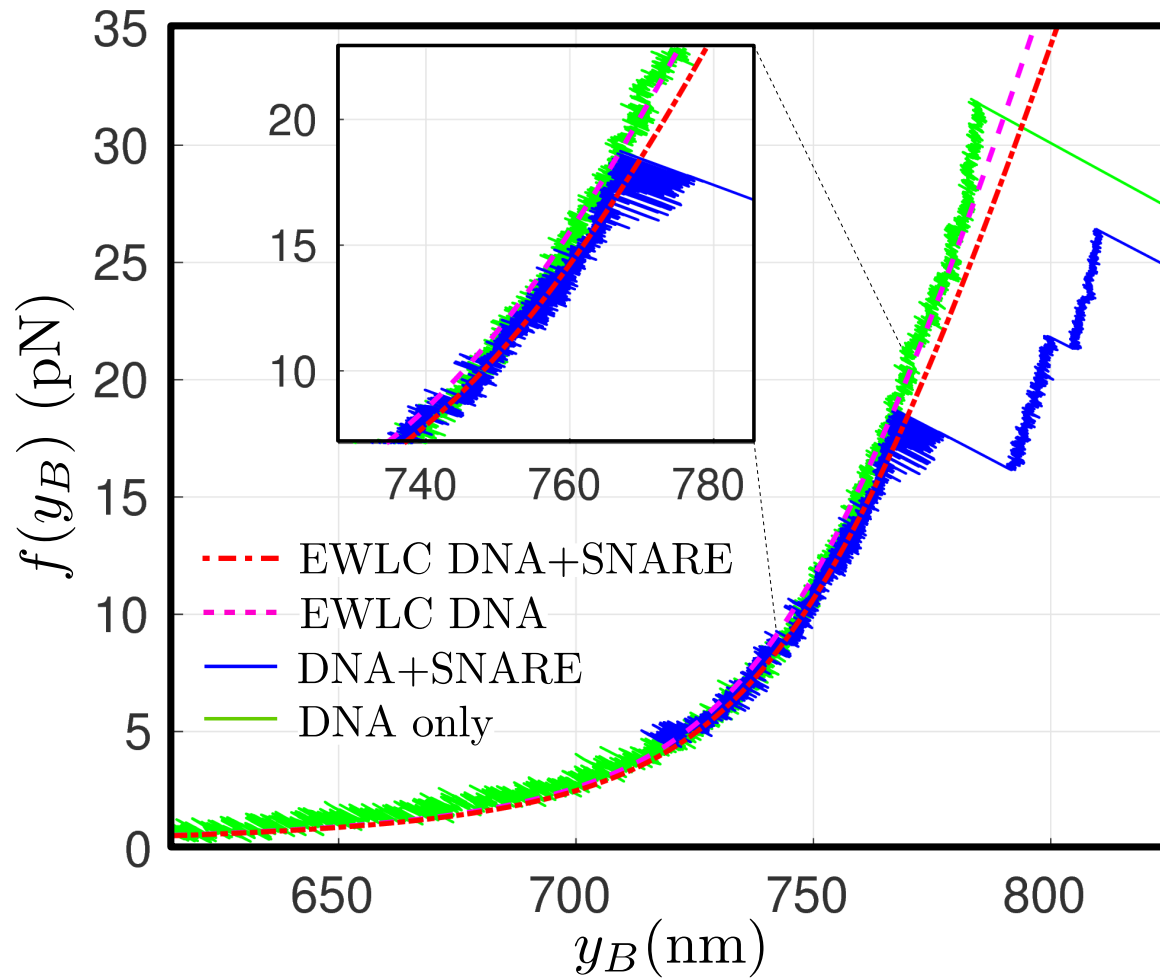


**Fig. S1.** Force-extension curve of the SNARE-DNA conjugate of Ref. (1) (blue curve), and FEC of the DNA handle alone (green curve). The SNARE-DNA conjugate and the DNA alone FECs can be approximately fitted by the extended worm-like chain model (EWLC) reported in Eq. 4 (pink dashed line).

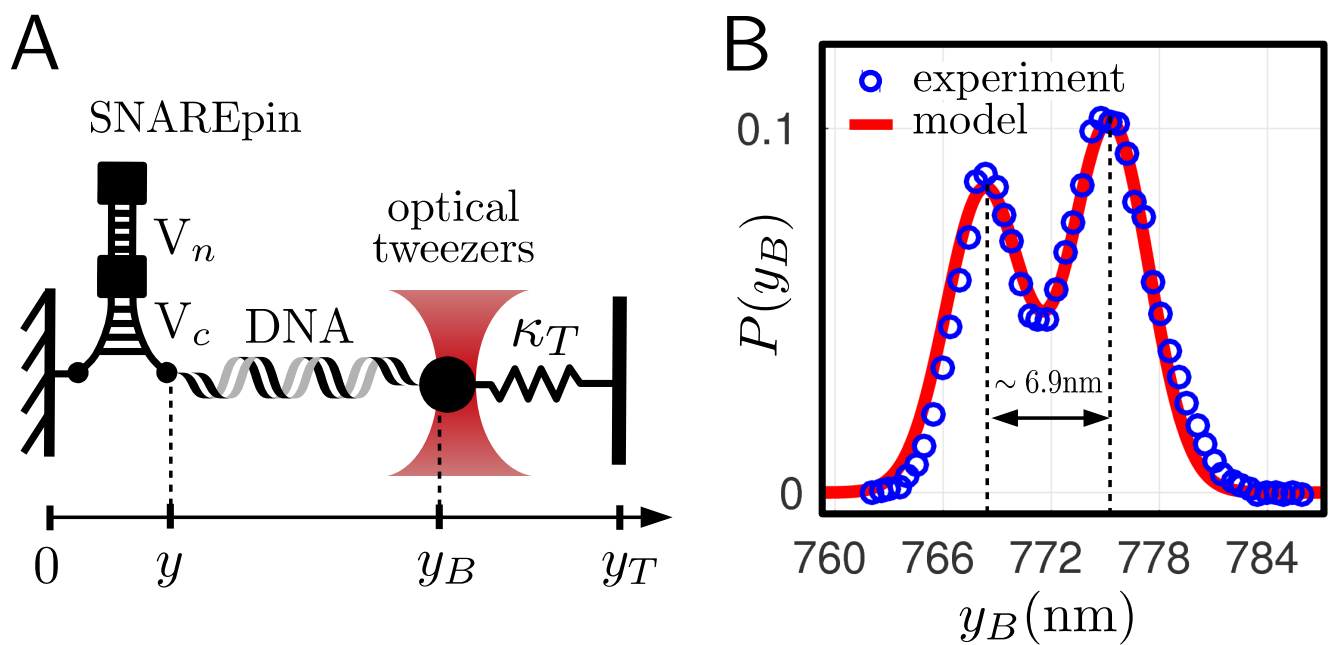


**Fig. S2.** Experimental setup and characterization of the unzipping and zippering of a single SNARE complex. (A) The SNARE complex is trapped to one side and linked to a DNA-handle, which is anchored to an optical-tweezers bead on the other side. Here,  $y_T$  denotes the total elongation of the system,  $y_B$  the position of the second bead and  $y$  the internal configuration of the SNAREpin. (B) The experimental probability density of the position of the bead  $y_B$  (open blue circles) of Ref. (1), fitted by the equilibrium model (solid red line).

## References

1. Gao Y, et al. (2012) Single reconstituted neuronal SNARE complexes zipper in three distinct stages. *Science* 337(6100):1340–1343.
2. Zhang Y (2017) Energetics, kinetics, and pathway of SNARE folding and assembly revealed by optical tweezers. *Protein Science* 26(7):1252–1265.
3. Moroz JD, Nelson P (1997) Torsional directed walks, entropic elasticity and dna twist stiffness. *Proc. Nat. Acad. Sci. USA*. 94:14418 –14422.
4. Bouchiat C, et al. (76) Estimating the persistence length of a worm-like chain molecule from force-extension measurements. *Biophys. J.* 1999:409–413.
5. Li F, Tiwari N, Rothman JE (2016) Kinetic barriers to SNAREpin assembly in the regulation of membrane docking/priming and fusion in *Proceedings of the . . .* (National Academy of Sciences), pp. 10536–10541.
6. Evans E (1991) Entropy-driven tension in vesicle membranes and unbinding of adherent vesicles. *Langmuir* 7(9):1900–1908.
7. Rand RP, Parsegian VA (1989) Hydration forces between phospholipid bilayers. *Biochimica et Biophysica Acta (BBA) - Reviews on Biomembranes* 988(3):351–376.
8. Leckband D, Israelachvili J (2001) Intermolecular forces in biology. *Q. Rev. Biophys.* 34(02):105–267.
9. Donaldson SH, Lee CT, Chmelka BF, Israelachvili JN (2011) General hydrophobic interaction potential for surfactant/lipid bilayers from direct force measurements between light-modulated bilayers. *PNAS* 108(38):15699–15704.
10. Ryham RJ, Klotz TS, Yao L, Cohen FS (2016) Calculating Transition Energy Barriers and Characterizing Activation States for Steps of Fusion. *Biophys. J.* 110(5):1110–1124.
11. Lentz BR, Lee J (2009) Poly(ethylene glycol) (PEG)-mediated fusion between pure lipid bilayers: a mechanism in common with viral fusion and secretory vesicle release? (Review). *Molecular Membrane Biology* 16(4):279–296.
12. Zhang Z, Jackson MB (2008) Temperature Dependence of Fusion Kinetics and Fusion Pores in Ca<sup>2+</sup>-triggered Exocytosis from PC12 Cells. *J. Gen. Physiol.* 131(2):117–124.
13. Cohen FS, Melikyan GB (2004) The Energetics of Membrane Fusion from Binding, through Hemifusion, Pore Formation, and Pore Enlargement. *Journal of Membrane Biology* 199(1):1–14.
14. Mostafavi H, et al. (2017) Entropic forces drive self-organization and membrane fusion by SNARE proteins. *Proc. Nat. Acad. Sci. U.S.A.* 84(21):201611506–5460.
15. François-Martin C, Rothman JE, Pincet F (2017) Low energy cost for optimal speed and control of membrane fusion. *PNAS* 114(6):1238–1241.
16. Markvoort AJ, Marrink SJ (2011) Lipid acrobatics in the membrane fusion arena. *Curr Top Membr* 68:259–294.
17. Finkelstein A, Zimmerberg J, Cohen FS (1986) Osmotic swelling of vesicles: its role in the fusion of vesicles with planar phospholipid bilayer membranes and its possible role in exocytosis. *Annual Review of Physiology* 48(1):163–174.
18. Grafmüller A, Shillcock J, Lipowsky R (2007) Pathway of membrane fusion with two tension-dependent energy barriers. *Physical review letters* 98(21):218101.
19. Grafmüller A, Shillcock J, Lipowsky R (2009) The fusion of membranes and vesicles: pathway and energy barriers from dissipative particle dynamics. *Biophysical journal* 96(7):2658–2675.
20. Lee JY, Schick M (2009) Calculation of free energy barriers to the fusion of small vesicles. *Biophysical journal* 94(5):1699–1706.
21. Xu W, et al. (2016) A Programmable DNA Origami Platform to Organize SNAREs for Membrane Fusion. *J. Am. Chem. Soc.* 138(13):4439–4447.
22. Domanska MK, Kiessling V, Stein A, Fasshauer D, Tamm LK (2009) Single Vesicle Millisecond Fusion Kinetics Reveals Number of SNARE Complexes Optimal for Fast SNARE-mediated Membrane Fusion. *J. Biol. Chem.* 284(46):32158–32166.
23. Risken H (1988) *The Fokker-Planck equation Methods of solution and application.* (Springer).